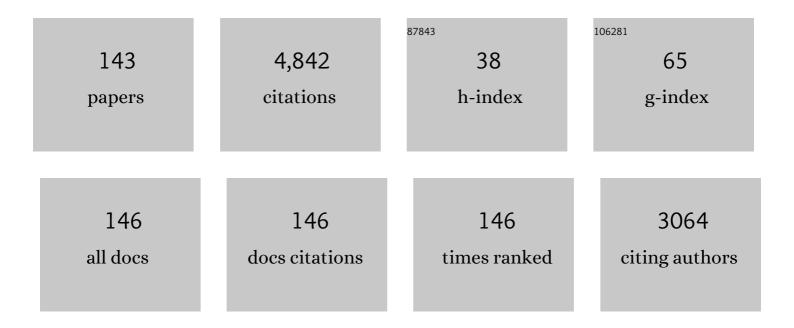
## Robin Schaeublin

List of Publications by Year in descending order

Source: https://exaly.com/author-pdf/6405386/publications.pdf Version: 2024-02-01



#	Article	IF	CITATIONS
1	Present development status of EUROFER and ODS-EUROFER for application in blanket concepts. Fusion Engineering and Design, 2005, 75-79, 989-996.	1.0	412
2	The microstructure and associated tensile properties of irradiated fcc and bcc metals. Journal of Nuclear Materials, 2000, 276, 114-122.	1.3	303
3	Deformation behaviour and microstructure of nanocrystalline electrodeposited and high pressure torsioned nickel. Acta Materialia, 2005, 53, 2337-2349.	3.8	193
4	Impact of irradiation on the microstructure of nanocrystalline materials. Journal of Nuclear Materials, 2004, 329-333, 953-957.	1.3	186
5	Review on the EFDA programme on tungsten materials technology and science. Journal of Nuclear Materials, 2011, 417, 463-467.	1.3	157
6	On the potentiality of using ferritic/martensitic steels as structural materials for fusion reactors. Nuclear Fusion, 2004, 44, 56-61.	1.6	119
7	Effect of helium on irradiation-induced hardening of iron: A simulation point of view. Journal of Nuclear Materials, 2007, 362, 152-160.	1.3	109
8	Microstructure and mechanical properties of two ODS ferritic/martensitic steels. Journal of Nuclear Materials, 2002, 307-311, 778-782.	1.3	104
9	Laser additive manufacturing of biodegradable magnesium alloy WE43: A detailed microstructure analysis. Acta Biomaterialia, 2019, 98, 36-49.	4.1	103
10	Impact of He and Cr on defect accumulation in ion-irradiated ultrahigh-purity Fe(Cr) alloys. Acta Materialia, 2013, 61, 6958-6971.	3.8	102
11	W–2 wt.%Y2O3 composite: Microstructure and mechanical properties. Materials Science & Engineering A: Structural Materials: Properties, Microstructure and Processing, 2012, 538, 53-57.	2.6	99
12	Microstructural development under irradiation in European ODS ferritic/martensitic steels. Journal of Nuclear Materials, 2006, 351, 247-260.	1.3	91
13	Irradiation-induced stacking fault tetrahedra in fcc metals. Philosophical Magazine, 2005, 85, 769-777.	0.7	85
14	Effects of irradiation on the microstructure and mechanical properties of nanostructured materials. Philosophical Magazine, 2005, 85, 723-735.	0.7	84
15	A method for simulating electron microscope dislocation images. Materials Science & Engineering A: Structural Materials: Properties, Microstructure and Processing, 1993, 164, 373-378.	2.6	80
16	MD modeling of defects in Fe and their interactions. Journal of Nuclear Materials, 2003, 323, 181-191.	1.3	72
17	The EU programme for modelling radiation effects in fusion reactor materials: An overview of recent advances and future goals. Journal of Nuclear Materials, 2009, 386-388, 1-7.	1.3	68
18	Methods for determining precise values of antiphase boundary energies in Ni <sub>3</sub> Al. Philosophical Magazine Letters, 1991, 64, 327-334.	0.5	62

#	Article	IF	CITATIONS
19	Microstructure of irradiated ferritic/martensitic steels in relation to mechanical properties. Journal of Nuclear Materials, 2002, 307-311, 197-202.	1.3	62
20	Mechanical behaviour of nanocrystalline electrodeposited Ni above room temperature. Scripta Materialia, 2005, 53, 23-27.	2.6	61
21	Compositional Grading for Efficient and Narrowband Emission in CdSe-Based Core/Shell Nanoplatelets. Chemistry of Materials, 2019, 31, 9567-9578.	3.2	59
22	Molecular dynamics simulation of radiation damage in bcc tungsten. Journal of Nuclear Materials, 2009, 386-388, 97-101.	1.3	58
23	Investigation of microstructure and mechanical properties of W–Y and W–Y2O3 materials fabricated by powder metallurgy method. International Journal of Refractory Metals and Hard Materials, 2015, 50, 210-216.	1.7	56
24	Helium and point defect accumulation: (i) microstructure and mechanical behaviour. Comptes Rendus Physique, 2008, 9, 389-400.	0.3	52
25	Vibrational contributions to the stability of point defects in bcc iron: A first-principles study. Nuclear Instruments & Methods in Physics Research B, 2009, 267, 3009-3012.	0.6	50
26	Comparison between bulk and thin foil ion irradiation of ultra high purity Fe. Journal of Nuclear Materials, 2013, 442, S786-S789.	1.3	49
27	Tensile properties and microstructure of 590 MeV proton-irradiated pure Fe and a Fe–Cr alloy. Journal of Nuclear Materials, 2000, 283-287, 483-487.	1.3	47
28	State of a pressurized helium bubble in iron. Europhysics Letters, 2009, 85, 60008.	0.7	47
29	Influence of the stress field due to pressurized nanometric He bubbles on the mobility of an edge dislocation in iron. Philosophical Magazine, 2010, 90, 1075-1100.	0.7	47
30	Effect of interatomic potential on the behavior of dislocation-defect interaction simulation in α-Fe. Journal of Nuclear Materials, 2008, 382, 147-153.	1.3	44
31	Helium effects on displacement cascades in α-iron. Journal of Physics Condensed Matter, 2008, 20, 415206.	0.7	43
32	Stability of helium bubbles in alpha-iron: A molecular dynamics study. Journal of Nuclear Materials, 2009, 386-388, 360-362.	1.3	43
33	Microstructure and mechanical properties of a W–2wt.%Y2O3 composite produced by sintering and hot forging. Journal of Nuclear Materials, 2013, 442, S225-S228.	1.3	43
34	Molecular dynamics simulation of radiation damage in bcc tungsten. Nuclear Instruments & Methods in Physics Research B, 2007, 255, 27-31.	0.6	42
35	Modelling irradiation effects in fusion materials. Fusion Engineering and Design, 2007, 82, 2413-2421.	1.0	40
36	Dislocation–void interaction in Fe: A comparison between molecular dynamics and dislocation dynamics. Journal of Nuclear Materials, 2009, 386-388, 102-105.	1.3	40

#	Article	IF	CITATIONS
37	Weak beam transmission electron microscopy imaging of superdislocations in ordered Ni3Al. Philosophical Magazine A: Physics of Condensed Matter, Structure, Defects and Mechanical Properties, 1996, 74, 113-136.	0.7	39
38	Multiscale modelling of bi-crystal grain boundaries in bcc iron. Journal of Nuclear Materials, 2009, 385, 262-267.	1.3	39
39	Surface-induced vacancy loops and damage dispersion in irradiated Fe thin films. Acta Materialia, 2015, 101, 22-30.	3.8	38
40	Microstructure assessment of the low activation ferritic/martensitic steel F82H. Journal of Nuclear Materials, 1998, 258-263, 1178-1182.	1.3	37
41	The effects of irradiation and testing temperature on tensile behaviour of stainless steels. Journal of Nuclear Materials, 2000, 283-287, 446-450.	1.3	37
42	The microstructure and tensile properties of pure Ni single crystal irradiated with high energy protons. Journal of Nuclear Materials, 2002, 307-311, 374-379.	1.3	37
43	Strengthening due to Cr-rich precipitates in Fe–Cr alloys: Effect of temperature and precipitate composition. Journal of Applied Physics, 2010, 107, .	1.1	37
44	Differences in the microstructure of the F82H ferritic/martensitic steel after proton and neutron irradiation. Journal of Nuclear Materials, 2000, 283-287, 339-343.	1.3	35
45	-Loop characterization in α-Fe: comparison between experiments and modeling. Journal of Nuclear Materials, 2002, 307-311, 871-875.	1.3	35
46	Analysis of high temperature deformation mechanism in ODS EUROFER97 alloy. Journal of Nuclear Materials, 2008, 382, 210-216.	1.3	35
47	Towards refining microstructures of biodegradable magnesium alloy WE43 by spark plasma sintering. Acta Biomaterialia, 2019, 98, 67-80.	4.1	35
48	Effect of mechanical alloying on the mechanical and microstructural properties of ODS EUROFER 97. Fusion Engineering and Design, 2007, 82, 2543-2549.	1.0	34
49	Molecular dynamics modeling of cavity strengthening in irradiated iron. Journal of Computer-Aided Materials Design, 2007, 14, 191-201.	0.7	33
50	Analysis of hardening limits of oxide dispersion strengthened steel. Journal of Nuclear Materials, 2013, 432, 323-333.	1.3	33
51	Evolution of the mechanical properties of the F82H ferritic/martensitic steel after 590 MeV proton irradiation. Journal of Nuclear Materials, 1998, 258-263, 1345-1349.	1.3	32
52	On the formation of stacking fault tetrahedra in irradiated austenitic stainless steels – A literature review. Journal of Nuclear Materials, 2013, 442, S761-S767.	1.3	29
53	Biocorrosion Zoomed In: Evidence for Dealloying of Nanometric Intermetallic Particles in Magnesium Alloys. Advanced Materials, 2019, 31, e1903080.	11.1	29
54	Radiation damage in ferritic/martensitic steels for fusion reactors: a simulation point of view. Nuclear Fusion, 2007, 47, 1690-1695.	1.6	27

#	Article	IF	CITATIONS
55	Irradiation induced behavior of pure Ni single crystal irradiated with high energy protons. Journal of Nuclear Materials, 2003, 323, 388-393.	1.3	26
56	Effect of irradiation on the microstructure and the mechanical properties of oxide dispersion strengthened low activation ferritic/martensitic steel. Journal of Nuclear Materials, 2007, 367-370, 217-221.	1.3	26
57	On the lattice coherency of oxide particles dispersed in EUROFER97. Journal of Nuclear Materials, 2009, 386-388, 515-519.	1.3	26
58	Exceptional Strengthening of Biodegradable Mg-Zn-Ca Alloys through High Pressure Torsion and Subsequent Heat Treatment. Materials, 2019, 12, 2460.	1.3	26
59	Stacking-fault mediated plasticity and strengthening in lean, rare-earth free magnesium alloys. Acta Materialia, 2021, 211, 116877.	3.8	26
60	The mechanical properties and microstructure of the OPTIMAX series of low activation ferritic–martensitic steels. Journal of Nuclear Materials, 2000, 283-287, 731-735.	1.3	25
61	Time-Resolved X-Ray Microtomography Observation of Intermetallic Formation Between Solid Fe and Liquid Al. Metallurgical and Materials Transactions A: Physical Metallurgy and Materials Science, 2013, 44, 4119-4123.	1.1	23
62	Nanometric crystal defects in transmission electron microscopy. Microscopy Research and Technique, 2006, 69, 305-316.	1.2	22
63	Chemical segregation behavior of the low activation ferritic/martensitic steel F82H. Journal of Nuclear Materials, 1998, 258-263, 1350-1355.	1.3	21
64	Microstructure and growth modes of stoichiometric NiAl and Ni 3 Al thin films deposited by r.fmagnetron sputtering. Thin Solid Films, 2000, 368, 26-34.	0.8	21
65	Atomistic simulations of nanometric dislocation loops in bcc tungsten. Nuclear Instruments & Methods in Physics Research B, 2009, 267, 3218-3222.	0.6	21
66	Atomistic simulation of the a0 ã€^100〉 binary junction formation and its unzipping in body-centered cubic iron. Acta Materialia, 2014, 64, 24-32.	3.8	20
67	Nano-sized prismatic vacancy dislocation loops and vacancy clusters in tungsten. Nuclear Materials and Energy, 2018, 16, 60-65.	0.6	20
68	Cascade overlap induced amorphization and disordering in irradiated intermetallics nial and Ni <sub>3</sub> Al: A molecular dynamic study. Radiation Effects and Defects in Solids, 1997, 141, 349-362.	0.4	19
69	Structure–mechanics relationships in proton irradiated pure titanium. Journal of Nuclear Materials, 2002, 307-311, 696-700.	1.3	19
70	Molecular dynamics study of strengthening by nanometric void and Cr alloying in Fe. Journal of Nuclear Materials, 2013, 442, S643-S648.	1.3	19
71	Structure of complex oxide nanoparticles in a Fe–14Cr–2W–0.3Ti–0.3Y2O3 ODS RAF steel. Journal of Nuclear Materials, 2013, 442, S158-S163.	1.3	19
72	Transmission electron microscopy contrast simulations of <100>-superdislocations in the L12 ordered structure. Scripta Materialia, 1998, 39, 1325-1332.	2.6	18

#	Article	IF	CITATIONS
73	Post-irradiation deformation in a Fe-9%Cr alloy. Materials Science & Engineering A: Structural Materials: Properties, Microstructure and Processing, 2001, 309-310, 82-86.	2.6	18
74	Microstructure of Ti5Al2.5Sn and Ti6Al4V deformed in tensile and fatigue tests. Journal of Nuclear Materials, 2002, 305, 52-59.	1.3	18
75	Interaction of irradiation-induced prismatic dislocation loops with free surfaces in tungsten. Nuclear Instruments & Methods in Physics Research B, 2017, 393, 186-189.	0.6	18
76	Dislocation defect interaction in irradiated Cu. Materials Science & Engineering A: Structural Materials: Properties, Microstructure and Processing, 2005, 400-401, 251-255.	2.6	16
77	Electron energy loss spectroscopy investigation through a nano ablated uranium dioxide sample. Talanta, 2013, 106, 408-413.	2.9	16
78	Quantitative analysis of CTEM images of small dislocation loops in Al and stacking fault tetrahedra in Cu generated by molecular dynamics simulation. Journal of Nuclear Materials, 2000, 276, 251-257.	1.3	15
79	Study of cascades damage in Ni by MD with different interatomic potentials. Journal of Nuclear Materials, 2007, 367-370, 298-304.	1.3	15
80	Synergistic effects of PKA and helium on primary damage formation in Fe–0.1%He. Journal of Nuclear Materials, 2007, 367-370, 462-467.	1.3	15
81	On the relationship between unusual mechanical properties and deformation substructures in ordered Ni3Al. Materials Science & Engineering A: Structural Materials: Properties, Microstructure and Processing, 1993, 164, 379-383.	2.6	14
82	Tensile properties of irradiated Cu single crystals and their temperature dependence. Journal of Nuclear Materials, 2004, 329-333, 1127-1132.	1.3	14
83	Temperature-controlled martensitic phase transformations in a model NiAl alloy. Journal of Applied Physics, 2006, 100, 063520.	1.1	14
84	Atomistic simulation of the influence of Cr on the mobility of the edge dislocation in Fe(Cr) alloys. Journal of Nuclear Materials, 2011, 417, 1094-1097.	1.3	14
85	Unconventional magnetization textures and domain-wall pinning in Sm–Co magnets. Scientific Reports, 2020, 10, 21209.	1.6	14
86	Plastic flow of martensitic model alloys. Materials Science & Engineering A: Structural Materials: Properties, Microstructure and Processing, 2004, 387-389, 16-21.	2.6	13
87	Fabrication of magnetic ring structures for Lorentz electron microscopy. Journal of Magnetism and Magnetic Materials, 2005, 290-291, 86-89.	1.0	13
88	Fabrication of curved-line nanostructures on membranes for transmission electron microscopy investigations of domain walls. Microelectronic Engineering, 2006, 83, 1726-1729.	1.1	13
89	Statistical analysis of oxides particles in ODS ferritic steel using advanced electron microscopy. Journal of Nuclear Materials, 2012, 422, 131-136.	1.3	13
90	Atomic-scale simulation of martensitic phase transformations in NiAl. Materials Science & Engineering A: Structural Materials: Properties, Microstructure and Processing, 2008, 481-482, 205-208.	2.6	12

#	Article	IF	CITATIONS
91	General dislocation image stress of anisotropic cubic thin film. Journal of Applied Physics, 2012, 112, 093522.	1.1	12
92	Selective ion-induced grain growth: Thermal spike modeling and its experimental validation. Acta Materialia, 2013, 61, 6171-6177.	3.8	12
93	Equilibrium ternary intermetallic phase in the Mg–Zn–Ca system. Journal of Materials Research, 2016, 31, 2147-2155.	1.2	11
94	Processing and characterization of a W–2Y material for fusion power reactors. Fusion Engineering and Design, 2011, 86, 2450-2453.	1.0	10
95	Advanced materials characterization and modeling using synchrotron, neutron, TEM, and novel micro-mechanical techniques—A European effort to accelerate fusion materials development. Journal of Nuclear Materials, 2013, 442, S834-S845.	1.3	10
96	Formation of an intermetallic phase by high energy implantation: The case of nickel in aluminum. Radiation Effects and Defects in Solids, 1993, 126, 185-188.	0.4	9
97	Welding-induced microstructure in austenitic stainless steels before and after neutron irradiation. Journal of Nuclear Materials, 2007, 360, 186-195.	1.3	9
98	Amorphization in Al induced by high-energy Ni ion implantation. Nuclear Instruments & Methods in Physics Research B, 1996, 107, 273-275.	0.6	7
99	Correlation of simulated TEM images with irradiation induced damage. Journal of Nuclear Materials, 2000, 283-287, 205-209.	1.3	7
100	Weak beam under convergent beam illumination. Ultramicroscopy, 2000, 83, 145-157.	0.8	7
101	Correlating TEM images of damage in irradiated materials to molecular dynamics simulations. Journal of Nuclear Materials, 2002, 307-311, 988-992.	1.3	7
102	Investigation of interfacial segregation at antiphase boundaries in a ternary alloy 84.8Ni–12.8Al–2.4Ta. Materials Science & Engineering A: Structural Materials: Properties, Microstructure and Processing, 2003, 360, 356-364.	2.6	7
103	The tensile properties of irradiated Ni single crystals and their temperature dependence. Philosophical Magazine, 2005, 85, 745-755.	0.7	7
104	Irradiation-induced phase transformation in undeformed and deformed NiTi shape memory thin films by high-energy ion beams. Philosophical Magazine, 2005, 85, 577-587.	0.7	7
105	The effect of point defects on the martensitic phase transformation. Materials Science & Engineering A: Structural Materials: Properties, Microstructure and Processing, 2006, 438-440, 102-108.	2.6	7
106	Atomistic simulation of He bubble in Fe as obstacle to dislocation. IOP Conference Series: Materials Science and Engineering, 2009, 3, 012013.	0.3	7
107	Effect of Thermal Treatments on Sn-Alloyed Al-Mg-Si Alloys. Materials, 2019, 12, 1801.	1.3	7
108	NANOSTRUCTURED TUNGSTEN-IRON ALLOY PREPARED BY ELECTRODEPOSITION. International Journal of Modern Physics B, 2006, 20, 4195-4200.	1.0	6

#	Article	IF	CITATIONS
109	Welding-induced mechanical properties in austenitic stainless steels before and after neutron irradiation. Journal of Nuclear Materials, 2007, 360, 255-264.	1.3	6
110	<i>In situ</i> transmission electron microscopy of the interaction between a moving dislocation and obstacles of dislocation character in pure iron. Philosophical Magazine Letters, 2013, 93, 575-582.	0.5	6
111	Assessment of convergence effects in weak-beam transmission electron microscopy in partial spacing measurements in Ni3Al. Philosophical Magazine Letters, 1997, 75, 179-186.	0.5	5
112	Structure analysis by diffraction of amorphous zones created by Ni ion implantation into pure Al. Ultramicroscopy, 2000, 83, 179-191.	0.8	5
113	Quantitative long-range-order measurement and disordering efficiency estimation in ion-irradiated bulk Ni3Al using cross-sectional conventional transmission electron microscopy. Applied Physics Letters, 2000, 77, 2680-2682.	1.5	5
114	From materials development to their test in IFMIF: an overview. Nuclear Fusion, 2011, 51, 113006.	1.6	5
115	Obstacle strength of binary junction due to dislocation dipole formation: An in-situ transmission electron microscopy study. Journal of Nuclear Materials, 2015, 465, 648-652.	1.3	5
116	On the Magnetism Behind the Besnus Transition in Monoclinic Pyrrhotite. Journal of Geophysical Research: Solid Earth, 2018, 123, 6236-6246.	1.4	5
117	The elasticity of the ½ a0 <111> and a0 <100> dislocation loop in α-Fe thin foil. Journal of Nuclear Materials, 2018, 510, 61-69.	1.3	5
118	Temperature dependence of magnetization processes in Sm(Co, Fe, Cu, Zr) <i>z</i> magnets with different nanoscale microstructures. Journal of Applied Physics, 2021, 129, .	1.1	5
119	Temperature dependence of irradiation effects in pure titanium. Philosophical Magazine, 2005, 85, 689-695.	0.7	4
120	Mechanical properties–microstructure correlation in neutron irradiated heat-affected zones of austenitic stainless steels. Journal of Nuclear Materials, 2007, 362, 287-292.	1.3	4
121	Stability of small vacancy clusters in tungsten by molecular dynamics. Nuclear Instruments & Methods in Physics Research B, 2020, 464, 56-59.	0.6	4
122	Atomic-Scale Characterization of Commensurate and Incommensurate Vacancy Superstructures in Natural Pyrrhotites. American Mineralogist, 2021, 106, 82-96.	0.9	4
123	Atomic structure evolution related to the Invar effect in Fe-based bulk metallic glasses. Nature Communications, 2022, 13, 1082.	5.8	4
124	Thermally Decomposed Binary Fe–Cr Alloys: Toward a Quantitative Relationship Between Strength and Structure. Advanced Engineering Materials, 2022, 24, .	1.6	4
125	SANS investigation of proton-irradiated EUROFER97. Journal of Nuclear Materials, 2004, 329-333, 289-293.	1.3	3
126	Surface damage in TEM thick α-Fe samples by implantation with 150 keV Fe ions. Nuclear Instruments & Methods in Physics Research B, 2015, 352, 217-220.	0.6	3

#	Article	IF	CITATIONS
127	Molecular dynamics simulations of phase formation and stability in the Al(Ni) system under irradiation. Philosophical Magazine, 2005, 85, 737-743.	0.7	2
128	Atomistic Simulation of ½<111> Screw Dislocations in BCC Tungsten. Advanced Materials Research, 0, 59, 247-252.	0.3	2
129	Molecular dynamics simulations of irradiation of α-Fe thin films with energetic Fe ions under channeling conditions. Journal of Nuclear Materials, 2014, 452, 453-456.	1.3	2
130	Hardening Mechanisms in Ferritic/Martensitic Steels. , 2004, , 341-351.		2
131	Thermally Decomposed Binary Fe–Cr Alloys: Toward a Quantitative Relationship Between Strength and Structure. Advanced Engineering Materials, 0, , 2100909.	1.6	2
132	A channeling goniometer with a wide temperature range sample holder. Nuclear Instruments & Methods in Physics Research B, 1992, 68, 249-252.	0.6	1
133	Stability of Al0.75Ni0.25 amorphous zones induced by Ni ion implantation into pure aluminium. Nuclear Instruments & Methods in Physics Research B, 1998, 146, 238-243.	0.6	1
134	Transformation de phase dans l'aluminium induite par implantation ionique de nickel à haute énergie. European Physical Journal Special Topics, 1994, 04, C3-297-C3-303.	0.2	1
135	Nickel ion irradiation of plasitically deformed martensitic titanium nickel thin films. European Physical Journal Special Topics, 2003, 112, 865-868.	0.2	1
136	Post-Irradiation Deformation Microstructures in Fe-9Cr. , 2001, , 523-534.		1
137	Bubble Microstructures in Helium Injected Palladium Foils. , 2004, , 492-501.		1
138	High Temperature Grain Boundary Internal Friction and Intergranular Precipitates in Ni-Cr Alloys. Materials Science Forum, 1996, 207-209, 789-792.	0.3	0
139	Relaxation mechanisms in martensitic NiTi(Cu): Internal friction measurements correlated to <i>in situ</i> TEM straining. Materials Science and Technology, 2008, 24, 913-919.	0.8	0
140	Comparison of conventional and Lorentz transmission electron microscopy in magnetic imaging of permanent magnets. Applied Physics Letters, 2021, 119, 022401.	1.5	0
141	Approach of He/dpa Synergistic Effects in Iron-Based Materials Using JANNUS. , 2013, , 111-122.		0
142	Characterizing faulted dipoles in TiAl with electron microscopy and computed image simulations. European Physical Journal Special Topics, 1993, 03, C7-441-C7-444.	0.2	0
143	Examination of Postirradiation Deformation Microstructures in F82H. , 2004, , 401-407.		0